



International Journal of Information and Communication Technology

ISSN online: 1741-8070 - ISSN print: 1466-6642

<https://www.inderscience.com/ijict>

A health prediction method for new energy vehicle power batteries based on AACNN-LSTM neural network

Jijun Zhang, Wenjian Feng, Yisong Tan, Hanping Pan

DOI: [10.1504/IJICT.2024.10063210](https://doi.org/10.1504/IJICT.2024.10063210)

Article History:

Received:	11 December 2023
Last revised:	25 December 2023
Accepted:	29 December 2023
Published online:	03 May 2024

A health prediction method for new energy vehicle power batteries based on AACNN-LSTM neural network

Jijun Zhang, Wenjian Feng, Yisong Tan and Hanping Pan*

College of Automotive and Information Engineering,
Guangxi Eco-Engineering Vocational & Technical College,
Liuzhou 545004, Guangxi, China

Email: zhang.jijun@163.com

Email: fwjian@163.com

Email: newagesong@163.com

Email: 15878292827@163.com

*Corresponding author

Abstract: Battery pack is an important part of the energy system of electric vehicles, and ensuring its safety is of great significance to the intelligent development of electric vehicles and human life and property. Detecting and ensuring the safety of battery pack in the energy system has become a research hotspot in the field of power batteries. This paper proposes a new composite deep neural network attention after CNN-LSTM (AACNN-LSTM) based on the characteristics and limitations of long- and short-term memory (LSTM) neural network, one-dimensional convolution neural network (1D-CNN) and other methods. We have carried out comparative experiments such as data division of different life stages, ablation experiments of multiple architecture combinations, and comparison with different types of algorithms. The results show that compared with other methods, the precision is significantly improved and the operation efficiency is maintained. Finally, the proposed health state estimation method is verified by three different battery accelerated aging test datasets. The experimental results show that the proposed method shows excellent battery health state estimation performance and good robustness under different working conditions and different number of training cycles.

Keywords: life prediction; attention mechanism; time series prediction; LSTM.

Reference to this paper should be made as follows: Zhang, J., Feng, W., Tan, Y. and Pan, H. (2024) 'A health prediction method for new energy vehicle power batteries based on AACNN-LSTM neural network', *Int. J. Information and Communication Technology*, Vol. 24, No. 5, pp.74–94.

Biographical notes: Jijun Zhang is a University Lecturer, graduated from Guilin University of Electronic Technology with a Master's in Engineering in 2015, and currently works in Guangxi Eco-Engineering Vocational and Technical College. His research direction is new energy vehicle technology, automotive manufacturing and testing technology. He presided over four projects and published five papers publicly, demonstrating strong research and teaching abilities.

Wenjian Feng is a Professor who graduated from Xidian University in 2009 with a degree in engineering, and currently works in Guangxi Eco-Engineering Vocational and Technical College. His research direction is algorithm optimisation and big data technology. He presided over 15 projects, obtained six computer software copyrights, two utility model patents, three invention patents, published 13 papers, of which four were published as the first author or corresponding author. He has strong scientific research ability and teaching ability.

Yisong Tan is a full-time teacher and graduated from Dalian University of Technology with a Master's degree in Engineering in 2009. He is currently employed at Guangxi Eco-Engineering Vocational and Technical College, with a research focus on the application of artificial intelligence technology.

Hanping Pan is a University Lecturer, graduated from Guangxi University of Science and Technology with a Bachelor's degree in Engineering in 2012, and currently works in Guangxi Eco-Engineering Vocational and Technical College. His research direction is new energy vehicle technology, automotive manufacturing and testing technology. He presided over three projects and published 11 papers publicly, obtained two utility model patents, demonstrating strong research and teaching abilities.

1 Introduction

Lithium-ion batteries have been widely used in portable consumer electronics and high-power electric vehicles because of their excellent energy density, high working voltage and low self-discharge rate (Zhou et al., 2022). The endurance of lithium battery is directly linked to the energy density; however, high energy density is also accompanied by high risk (Xue et al., 2022). In the field of consumer electronics, thermal runaway of the battery pack of the energy system is one of its biggest problems. Considering that electric vehicles work in a complex environment, how to ensure the reliability and safety of the battery pack will be a huge challenge. Overcharge and discharge, sensor fault, external short circuit (ESC), internal short circuit (ISC) and other problems are common faults in lithium-ion battery pack fault (Wang et al., 2022). Short-circuit fault is more dangerous than overcharge and discharge fault. Short-circuit fault is usually accompanied by abnormally high heating rate, which is easy to lead to runaway heating. The runaway of one battery will affect the safe operation of adjacent batteries and further trigger the chain exothermic reaction (Liu, 2022). In the short circuit fault, the ISC is considered to be one of the most fundamental reasons for the thermal runaway of the battery pack (Wang, 2022b). Therefore, it is very necessary to study the ISC of the battery pack.

Data-driven prediction methods use potential features extracted from actual monitoring data to predict performance degradation trends, mainly including statistical analysis methods (Zhang, 2022) and machine learning methods (Wang, 2022a). Statistical analysis methods usually use statistical models or random processes to establish the relationship model between battery monitoring indicators and performance degradation, involving parameter estimation to obtain relevant statistical information such as probability (Wei et al., 2022) density, which requires relatively ideal assumptions and is prone to risk of information loss.

The machine learning method does not need to build a specific degradation model, and usually uses the original monitoring data for feature extraction and training to directly obtain the prediction results. However, the traditional machine learning methods have different ability of model fitting, and the workload of model selection is large. Especially for the multi-dimensional time series prediction problem of PEMFC (Liu, 2022) life prediction, there are complex nonlinear relationships between the characteristics of each dimension and between each time step, and the original data often has problems such as noise and deviation. The traditional machine learning method cannot take these characteristics into account at the same time (Zhou, 2022), and the prediction accuracy needs to be improved.

The life prediction of PEMFC is based on the physical and chemical process (Liang, 2022), operation status, environmental conditions and working conditions of the battery to predict when to stop effective work or failure (Duan, 2021). However, in the process of battery operation, there are many factors that affect the life of the battery. The reasons for performance degradation include not only low temperature startup, cycle start and stop (Wang et al., 2021), temperature and humidity fluctuations, insufficient gas supply, insufficient humidification, diffusion layer flooding, overload work, etc., but also ‘single low’ and ‘low hydrogen’ will cause irreversible damage to the performance and life of the battery. Its effective life prediction faces great challenges (Tan and Wei, 2021) around these complex factors. The prediction methods involved in relevant research at home and abroad can be divided into model-driven methods and data-driven methods (Li et al., 2021).

The model-based observer method simulates the characteristics of battery capacity attenuation through the mathematical model of the battery, and further combines the model with advanced filtering algorithm to achieve accurate SOH estimation (Yao et al., 2021). The commonly used battery mathematical model includes the equivalent circuit model and the electrochemical model. The equivalent circuit model uses the basic electronic components to simulate the external output characteristics of the battery, while the electrochemical model describes the dynamic characteristics inside the battery through a series of complex partial differential equations (He, 2021). The equivalent circuit model usually uses the internal resistance growth of the battery to describe the SOH, such as Ze et al. (Liu, 2021) combined the second-order equivalent circuit model with the adaptive square root unscented Kalman filter algorithm to achieve the joint estimation of battery SOH and state of charge (SOC), but this model cannot directly describe the capacity decay or the change of internal characteristics of the battery. The electrochemical model can directly reflect the internal aging mechanism of the battery, such as the increase of solid electrolyte interface (SEI), lithium electroplating and the loss of active materials, and characterise the aging state of the battery from the perspective of electrochemistry (Zhang, 2021b). Lawder et al. (Qian, 2021) combined the pseudo-two-dimensional model of porous electrode with the side reaction of SEI formation to simulate the growth process of SEI film inside the battery. On this basis, the mathematical reconstruction method of the pseudo-two-dimensional model was applied to reduce the complexity of the model and reduce the calculation cost. The results show that the method is robust to various chemical components and battery types. The single-particle model is a simplification based on the full-order pseudo-two-dimensional model (Chen et al., 2020). By ignoring the kinetic equation in the electrolyte and assuming that the lithium ion concentration and potential in the electrolyte phase remain unchanged, the calculation cost is greatly reduced. Li et al. (Zhou and Wang, 2020)

proposed a battery aging model combining lithium ion loss model and single particle model, which realised rapid capacity prediction with the number of cycles and temperature changes, and also provided quantitative information on the formation and expansion of SEI film, as well as the resulting battery capacity degradation and power loss, which can be directly applied to the battery SOH estimation. The above model-based method has high accuracy and can describe the internal and external characteristics of the battery, but its equivalent circuit model is difficult to describe the capacity characteristics of the battery, while the electrochemical model is limited by complex partial differential equations and highly coupled model parameters, which makes its solution more difficult, so the model-based method is difficult to get practical application.

To sum up, this paper proposes an algorithm based on improved firefly algorithm to optimise BP neural network to estimate the health status of lithium batteries, optimises the steps of firefly movement in the firefly algorithm through Levy flight, and uses NASA Ames Research Center dataset to train and predict the algorithm, and evaluate the estimation effect of the algorithm.

2 Method and principle

2.1 ISC fault detection algorithm of battery pack based on Spearman rank correlation and TBi-GRU neural network

As shown in Figure 1, the TBi-GRU model used in this paper is composed of three parallel bi-GRU (bidirectional gating current unit, bi-GRU) models with 1D convolution. The number of 1D convolutions is mainly determined by considering the size of the model and through actual experiments. The model has n inputs, and each layer of bi-GRU has 64,128 hidden neural units, one dropout layer, and the output layer predicts n values. The convolution layer is mainly used to extract the local feature information of the feature time series, and bi-GRU is used to obtain the long-distance dependency relationship in the sequence.

- 1 Convolution layer. The convolution layer uses the convolution check to convolution the input time series to obtain the local feature information of the time series and the time series matrix after feature extraction $H \in R^{k \times n}$, among k is the length of the time series, n is the number of battery cells of the battery pack, and the convolution core S defined as $S \in R^{w \times n}$, w . The size of the convolution kernel, which is calculated as

$$y_i = f(S \cdot H_{i:i+h-1} + c) \quad (1)$$

Among, y_i represents the second feature of the time series output by convolution. c is offset, \cdot is the dot product of matrix. f is the activation function. This article uses the LeakyReLUs activation function

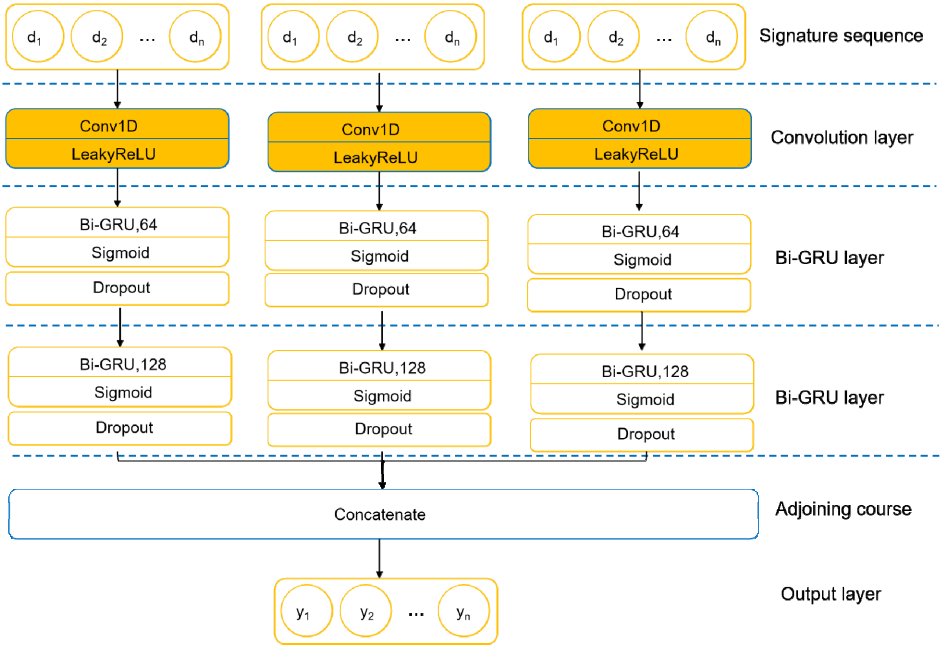
- 2 Bi-GRU layer. The bi-GRU used in this paper is composed of two gated recurrent unit (GRU) with the same structure (Hou and Fan, 2020) connected in reverse sequence. It divides the neurons in the GRU network into forward layer and backward layer. In terms of time, it considers both the information on the positive time axis (Hou and Fan, 2020) and the information on the negative time axis. The bi-GRU network structure is defined by formula (4). In general, the performance of

GRU and long- and short-term memory (LSTM) is similar (Ruan, 2020), but since the units in GRU can control the flow of information through reset and update gates, compared with LSTM, which needs forgetting gates, input gates and output gates, GRU has fewer parameters, and training is easier to converge, which can effectively reduce the training time.

$$h_t = \begin{cases} z_t = \sigma(W_z x_t + U_z h_{t-1} + b_z) \\ r_t = \sigma(W_r x_t + U_r h_{t-1} + b_r) \\ \tilde{h}_t = \tanh(W_h x_t + U_h (r_t \circ h_{t-1}) + b_h) \\ h_t = (1 - z_t) \circ \tilde{h}_t + z_t \circ h_{t-1} \end{cases} \quad (2)$$

Among, h_t on behalf of t the corresponding state of time can be divided into forward and backward in Bi-GRU, z_t, r_t represents the update door and reset door, \circ is the Hadamard product, W_r, W_h, U_z, U_r, U_h represent the parameter matrix and cycle matrix of the model respectively. b_z, b_r, b_h is the offset vector, σ represents sigmoid function, and \tanh represents hyperbolic tangent function.

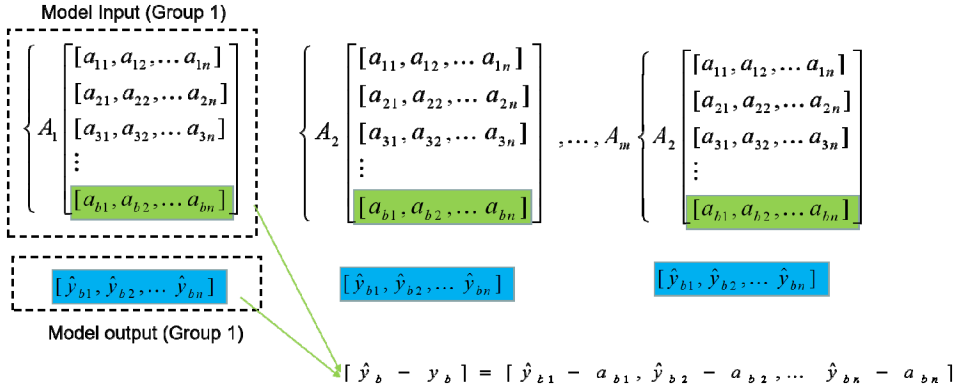
Figure 1 Model network structure (see online version for colours)



As shown in Figure 2, multi-dimensional time series A_m , group is m dimension is n , Count Reg b, m . The length of represents both m each group of battery data is processed $[a_b = a_{b1}, a_{b2}, \dots, a_{bn}]$ with b data for channels, $[a_b = a_{b1}, a_{b2}, \dots, a_{bn}]$. The data in corresponds to the extracted feature sequence. Length b it determines the number of models from input to prediction. During training, the loss is calculated using the input and current output of the next time point. During testing, the difference between the output of the model and the input of the current time is used to calculate the predicted

model anomaly detection results, and the baseline threshold is calculated and recorded. In practice, independent modelling is needed for the input data of each battery pack to facilitate the fine-tuning of each model in the later stage. Because the number of batteries in each battery pack is not the same, the time required for training to reach our needs is also different. Independent training can prevent the occurrence of some model over-fitting phenomenon.

Figure 2 Calculation process of input and output of visual model (see online version for colours)



In this paper, the process of fault detection is divided into three stages, namely, the process of fault prediction based on TBi-GRU model, the process of fault detection based on multi-channel optimisation and the process of fault location based on the results of detection (Lu, 2020). The detection process is shown in Figure 5.

- 1 Phase 1. Fault prediction. Fault characteristics to be detected y as the input of the model, obtain the prediction results y_{pre} . Calculate the prediction error according to formula (5) y_{error} . Then calculate the dynamic threshold according to the mean and standard deviation of the prediction error (Xu, 2020).

$$y_{error} = y - y_{pre} \tag{3}$$

- 2 Phase 2. Multi-channel optimisation. Multi-channel optimisation algorithm refers to the fusion of the detection results of different battery packs (Li, 2020b), and the correction of the prediction results based on certain rules to reduce false positives. The rules are as follows.
 - a There is only one ISC fault of multiple battery packs of electric vehicles in the same detection period (Wang, 2020).
 - b In the same group, there is no large number of abnormalities with similar amplitude in the same detection period. It should be noted that when only single battery pack detection is performed (Li, 2020a), it only executes rule.
 - b The model proposed in this paper can generate multiple models for all groups independently (Ovshinsky et al., 1993), the model can be upgraded and replaced freely, and each model can independently output results for test data, and the results of each channel can be fused on the basis of dynamic threshold to obtain the overall optimal.

- 3 Phase 3. Fault location (Zheng et al., 2019). Based on the threshold th of multi-channel optimisation, obtain the time of ISC occurrence $Time_{ISC}$ according to formula (6).

$$Time_{ISC} = \{t \mid y_{error}(t) > th\} \quad (4)$$

According to formula (5), the result is the serial number of the battery node with abnormal storage characteristics i and failure time t , $Cell_i(t) \in y_{error}(t)$ is the correlation between one battery cell and the next battery cell in the battery pack.

$$result = \{i, t \mid t \in Time_{ISC} \ \&\& \ Cell_i(t) > th\} \quad (5)$$

If the ISC fault occurs to the no. 3 battery cell, the characteristic Cell3 of no. 3 and no. 4 will increase, and the characteristic Cell2 of no. 2 and no. 3 will also increase. By finding two increased fault trends, the algorithm can distinguish the specific faulty battery cells in the lithium-ion battery pack for early warning. If multiple batteries fail at the same time, this method is still valid.

Based on the prediction results, the abnormal area of ISC is divided in the original data, and an unsupervised dynamic threshold calculation method is proposed based on the threshold calculation method of three standard deviations (Chen et al., 2019a). The calculation process is

$$th = \lambda(\mu_{train}(err_i) + 3 \times \sigma_{train}(err_i)) \quad (6)$$

where th is the threshold to be calculated, $(\mu_{train}(err_i))$ is the mean value of prediction error in training, $\sigma_{train}(err_i)$ is the standard deviation of prediction error in training, λ is the dynamic coefficient, and its corresponding mathematical expression is

$$\left. \begin{aligned} A &= \mu_{test}(err_i) / \mu_{train}(err_i) \\ B &= \sigma_{test}(err_i) / \sigma_{train}(err_i) \\ \lambda &= A \times 2 \leq B ? A : B \end{aligned} \right\} \quad (7)$$

Among, $\mu_{test}(err_i)$ $\sigma_{test}(err_i)$ represent the mean and standard deviation of the prediction error in the test, and the abnormal threshold λ with changes A . The ratio of the average value of storage test and training, Ratio of standard deviation between storage test and training.

2.2 Overall architecture mechanism of AACNN-LSTM model

According to the Chinese national standard GB/T 38914-2020, the evaluation criteria for the service life durability test of PEMFC for vehicles stipulates that the battery life is considered to be terminated when the average voltage of each cell is reduced by 10% under the reference current (Chen et al., 2019b). At the same time, PEMFC can obtain monitoring parameters from various sensors during operation, such as voltage, current, coolant temperature, air pressure, hydrogen pressure, stack humidity, etc. The change of each monitoring parameter may affect the output voltage of the battery. Moreover, the voltage attenuation of the battery does not change linearly, and its voltage does not change significantly in the early life, and only in the middle and late life will there be significant attenuation.

Figure 3 Main framework of the model

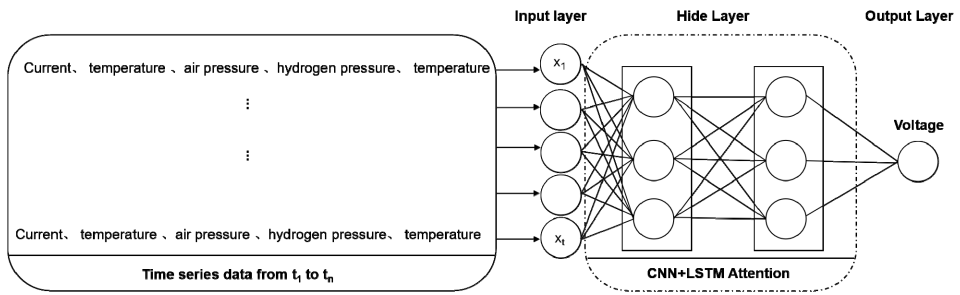
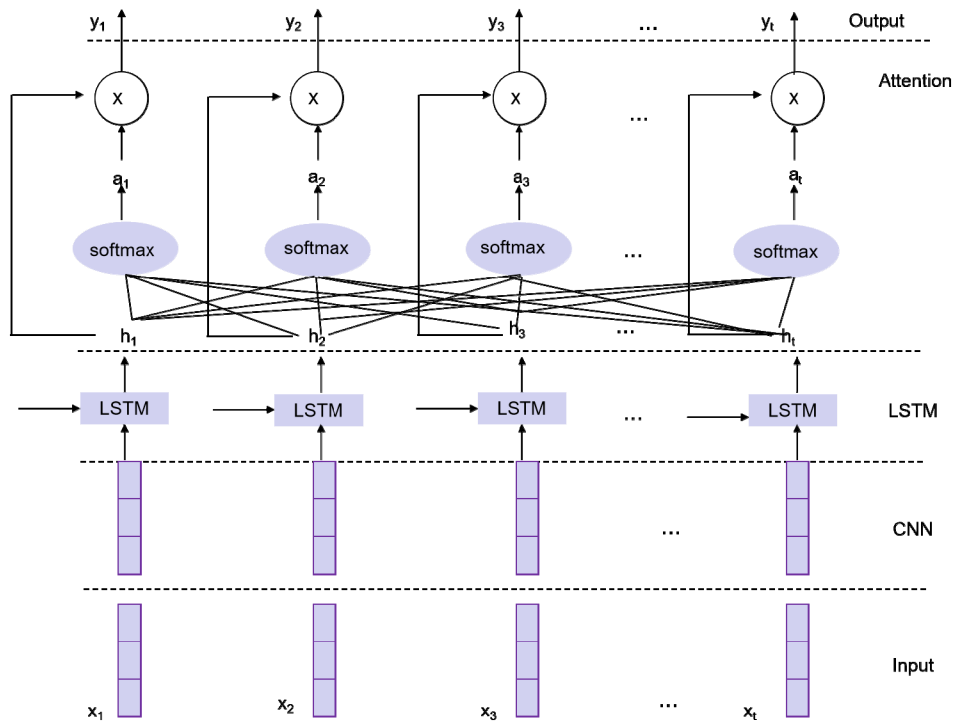


Figure 4 Attention after CNN-LSTM combination layer



In view of these characteristics of PEMFC, this paper proposes a multidimensional time series prediction model AACNN-LSTM based on CNN-LSTM-Attention (Chen, 2019) composite network. The overall architecture is shown in Figure 3. First, use 1D-CNN to smooth and filter, then use LSTM layer to learn the temporal relationship between multi-dimensional vectors, and finally introduce attention mechanism to conduct adaptive weighted learning of multi-dimensional vectors at different time steps from a global perspective, to determine which features play a key role in the prediction results. Finally, the model takes the output voltage of PEMFC as the prediction result for life assessment, and constructs an end-to-end depth regression model.

For multi-dimensional time series data, the ‘importance’ of each time step vector is different. Using the Attention mechanism, you can learn different weights of each vector. More importantly, you can adaptively learn dynamic weights in different contexts (each Attention vector is also multi-dimensional). The AACNN-LSTM proposed in this paper introduces this attention mechanism, and explores the effect of Attention location on the prediction performance of the model. The first is to set it after the feature extraction layer (i.e. CNNLSTM) of the model (before the output layer) (as shown in Figure 4). The input sequence is multiple sets of monitoring data vectors in the time window, expressed as x_1, x_2, \dots, x_t . As shown in Figure 3. The input sequence passes through CNN-LSTM to obtain the corresponding hidden layer vector h_1, h_2, \dots, h_t . Then input the attention layer and calculate the attention weight distribution value of each input a_1, a_2, \dots, a_t . So as to obtain new hidden layer features by weighting y_1, y_2, \dots, y_t . Finally, the sum of y_i is reduced to the prediction step size through the full connection layer, and the relu function is activated to obtain the prediction voltage v as the output of the model. Specifically described as:

$$h_i = LSTM(CNN(x_i)) \tag{8}$$

$$u_i = \tanh(W_q h_i + b_q) \tag{9}$$

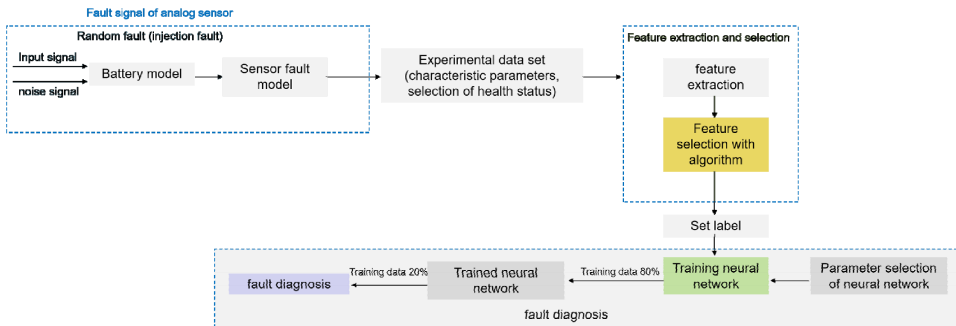
$$a_i = \frac{\exp(u_i^T u_s)}{\sum_{s=1}^t \exp(u_s^T u_s)} \tag{10}$$

$$y_i = a_i \otimes h_i \tag{11}$$

$$v = \text{relu}\left(\text{Dense}\left(\sum_{i=1}^t y_i\right)\right) \tag{12}$$

Among: W_q is a linear transformation matrix, b_q is the offset, both will be entered h_i convert to attention query vector u_i ; y_i is the product of vectors per element, and the result is still in vector form.

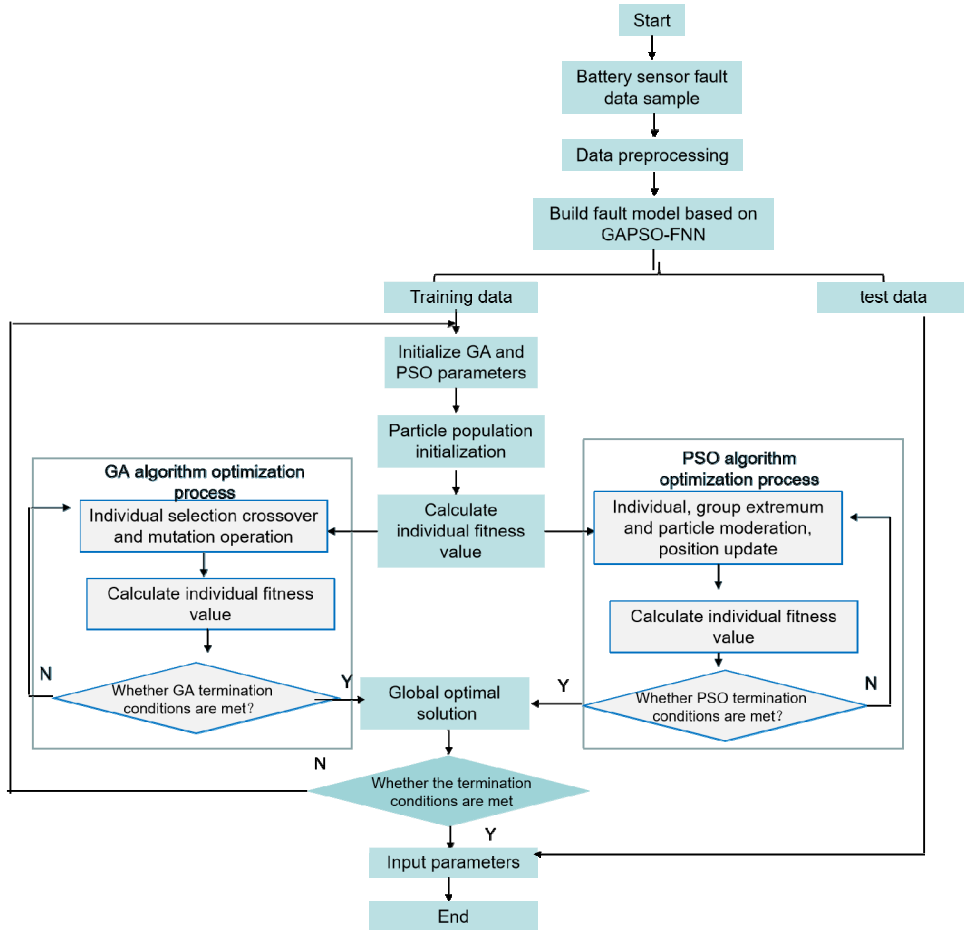
Figure 5 The flow chart of battery sensor fault diagnosis (see online version for colours)



2.3 Fault diagnosis of battery sensor based on GAPSO-FNN algorithm

The realisation of each function of the battery depends on the sensor inside the battery. If the sensor fails, it will cause the BMS (Li et al., 2019) to function abnormally and affect the safe and stable operation of the battery management system (Zeng, 2019). The sensor fault diagnosis of the battery is mainly divided into three parts, which are the battery sensor data acquisition, feature selection and extraction, and fault diagnosis. The battery sensor fault diagnosis process is shown in Figure 5.

Figure 6 Flow chart of GAPSO-FNN algorithm (see online version for colours)



Although the particle swarm optimisation algorithm has the advantages of small parameters and fast convergence speed, it is widely used in intelligent optimisation, but it is often limited because it is easy to fall into the local optimisation problem (Wang, 2019). In order to solve the local optimisation problem, the particle swarm optimisation algorithm based on genetic algorithm is introduced, which can help to jump out of the local optimisation and continue to search for other regions (Surya et al., 2021). The fuzzy neural network combines fuzzy reasoning and neural network (Li, 2019), has strong

self-learning ability and adaptive ability, and can continuously modify the membership function of fuzzy subsets. In order to have the adaptive ability and solve the local optimisation problem, this paper combines particle swarm optimisation and fuzzy neural network with genetic idea, which can not only improve the local search ability and the global search speed, but also realise the efficient use of the hybrid algorithm, making the hybrid algorithm more applicable to engineering practice. The algorithm flow chart of GAPSOFNN is shown in Figure 6. The GAPSO optimisation algorithm is composed of two parts: GA optimisation algorithm and PSO optimisation algorithm. This algorithm not only avoids the disadvantage of poor convergence of PSO algorithm, but also increases the information sharing mechanism between individuals, reducing the time spent in optimisation.

3 Experiment

3.1 Analysis of experimental data

The heat management system of PEMFC controls the heat balance in the reaction process, thus ensuring the stable working temperature of the stack. When the working environment temperature is low, the electrochemical reaction activity will decrease, resulting in an increase in impedance, and the overall performance of the stack will decline. However, if the temperature is too high, it will lead to catalyst degradation and battery softening (Liang, 2022; Duan, 2021). Therefore, temperature has a great influence on the output power and aging of PEMFC. It involves air temperature management and water heat management, and the main monitoring parameters are: hydrogen inlet temperature, hydrogen outlet temperature, air inlet temperature, and air outlet temperature; Circulating water outlet pressure, circulating water inlet pressure, hydrogen humidification temperature, air humidification temperature, cathode internal humidity, anode internal humidity, stack inlet water temperature, stack outlet water temperature, etc. Excessive anode differential pressure of PEMFC, high thermal conductivity of the stack, delayed response of the reaction gas, and blockage of the flow field may lead to under-gas phenomenon. Due to 'lack of oxygen', the hot area of the air inlet at the cathode side is higher than other parts of the bipolar plate, which leads to the aging of the membrane electrode. In serious cases, reverse electrode accidents will occur, which not only affects the service life, but also brings potential safety hazards (Liang, 2022; Duan, 2021). Generally speaking, the excess gas coefficient is the key factor affecting the performance of PEMFC. The efficiency of PEMFC power generation can be improved by accurately controlling the gas supply and hydrogen excess coefficient (the flow and proportion of air and hydrogen) of the stack, and the aging of membrane electrode caused by insufficient gas can be avoided at the same time. Therefore, the state of the reaction gas supply is closely related to the aging of PEMFC. The main monitoring parameters are: hydrogen inlet pressure, hydrogen outlet pressure, air inlet pressure, air outlet pressure, etc.

3.1.1 Feature selection

The data in this paper is from the bench life test of a PEMFC for three months. The monitoring parameters included in the data include: current density, hydrogen inlet pressure, hydrogen outlet pressure, air inlet pressure, air outlet pressure, circulating water outlet pressure, circulating water inlet pressure, hydrogen humidification temperature, air humidification temperature, cathode internal humidity, anode internal humidity, hydrogen inlet temperature, hydrogen outlet temperature, air inlet temperature, air outlet temperature, reactor inlet water temperature The water temperature at the stack outlet, etc.

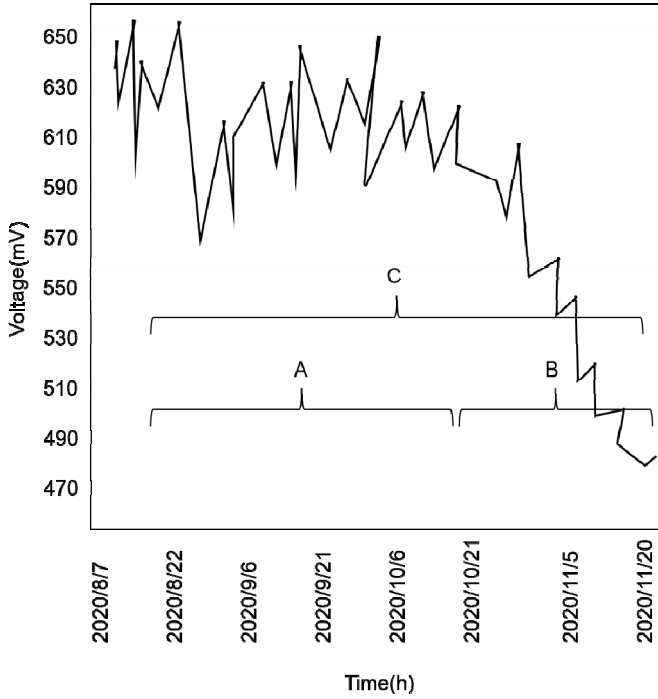
When the working conditions change, the chemical composition of the membrane electrode changes, the flow field of the bipolar plate changes, and the assembly pressure of the stack changes, the weight of each parameter on the life will change, making the prediction task more complex. Select some main monitoring parameters and draw the parameter correlation matrix shown in Figure 3 in the appendix, including voltage, air temperature difference, water temperature difference and air humidity. In the matrix, it can be found that the variation trend of the water temperature difference is the same as the attenuation trend of the battery voltage. Further draw the thermal diagram of water temperature difference and voltage, as shown in Figure 4 in the appendix. The ordinate is the water temperature difference, and the abscissa is the voltage, which more clearly shows this correlation.

Finally, based on the above correlation analysis and the lack of data, seven bottom monitoring parameters were selected as the dataset for research, which are: average voltage value of the stack, stack density, hydrogen stack inlet pressure, hydrogen stack outlet pressure, air stack inlet pressure, air stack outlet pressure, and circulating water outlet pressure. Among them, the average voltage value of the stack is used as the output result for life assessment, and the other is used as the feature (in the time series model, the historical average voltage is also used as the feature to predict the future average voltage).

3.1.2 Life interval division

The change of average battery voltage with time in the experimental dataset is shown in Figure 7. The ordinate is the average voltage, and the abscissa is the date and time. It can be seen that the broken line around 2020-10-15 has changed significantly. At before 2020-10-15, the average voltage of the battery changed around 620 mV, and the trend was stable. However, from 2020-10-15, the average voltage began to drop significantly, until it fell below 500 mV. In order to verify the applicability of the prediction model (whether the prediction accuracy of the model in different life stages of PEMFC meets the engineering needs), the data is divided into three intervals A, B, and C with 2020-10-15 as the dividing point. Interval A is before 2020-10-15 (early stage), interval B is after 2020-10-15 (middle and late stage), and interval C is the entire dataset.

Figure 7 Interval division of experimental dataset



3.2 Analysis of simulation results

When designing the battery sensor fault diagnosis scheme, we want the fitness value of the global optimal solution to be continuously reduced, even in the case of fewer iterations, it can reduce the battery sensor fault diagnosis time and significantly improve the accuracy, as shown in Figure 8. Because of the large difference between the centre temperature and the surface temperature of the battery, it is assumed that the temperature is at a fixed value (23). The results of the three fault diagnosis schemes are shown in Figure 9. As shown in Figures 10 and 11, the performance index comparison of the three fault diagnosis algorithms is shown in Table 1.

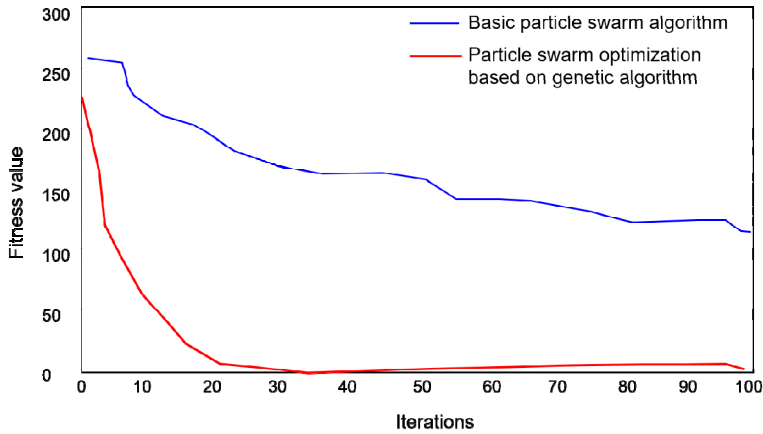
Table 1 Performance index comparison of three fault diagnosis algorithms

Name	Accuracy (%)	Specificity (%)	Accuracy (%)	Convergence time(s)
Traditional neural network algorithm	75.3	74.9	70.0	3.76
Fuzzy neural network algorithm	85.6	86.7	85.0	1.52
GAPSO-FNN algorithm	94.7	92.3	95.0	1.23

The input and output of the three algorithms in the above figure are the same, and the selection of input layer, hidden layer and output layer are also the same. As can be seen from Figure 9, the BP neural network cannot guarantee the global optimal value because

of its slow convergence speed and easy to fall into the local optimal value, so the actual value and the predicted value cannot completely coincide, and the error fluctuation is large. As can be seen from the confusion matrix, 30% of them are fault diagnosis errors. It can be seen from Figure 10 that the accuracy of fault diagnosis of fuzzy neural network is improved by 15% compared with BP neural network, and the training effect is good, which can well combine the empirical rules of expert system with neural network. It can be seen from Figure 11 and Table 1 that the GAPSO-fuzzy neural network algorithm incorporates the advantages of optimisation algorithm when training the model, which makes it adaptive and can ensure the global optimisation, and also makes the battery sensor fault diagnosis accuracy reach 95%, making the accuracy reach an ideal value.

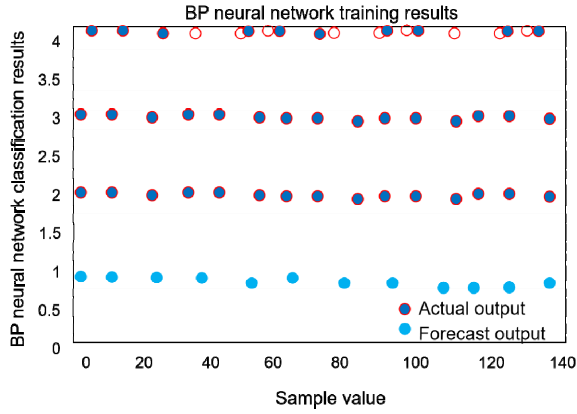
Figure 8 Optimisation results of GAPSO algorithm (see online version for colours)



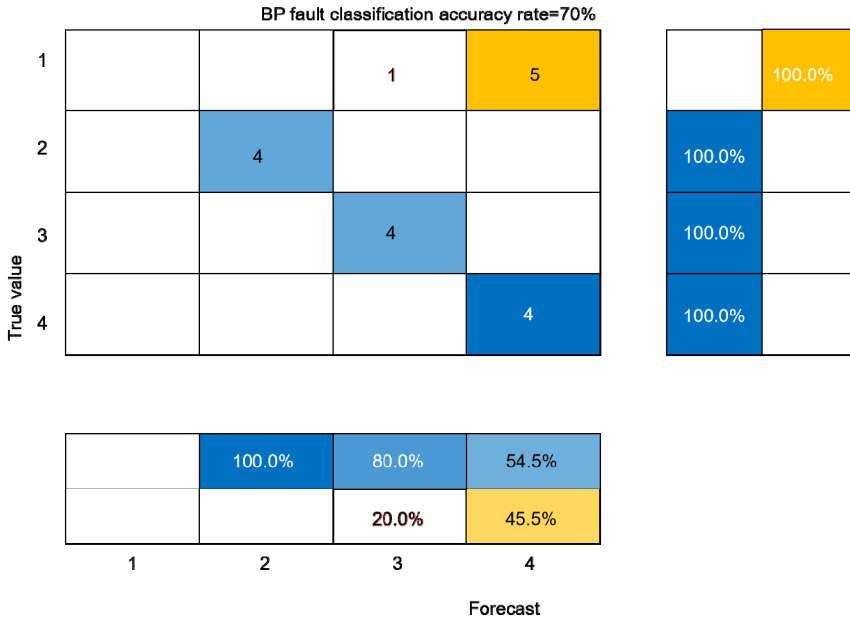
3.3 Robustness analysis

In order to analyse the robustness of the proposed SOH estimation method under different training cycles, the LSTM network is pre-trained with the first 1/2, 1/3 and 1/4 aging cycle data based on dataset 2, and the latter cycle data is used for SOH estimation. The experimental results are shown in Figure 12. The results of the training cycle show good consistency, and with the increase of the number of cycles, the SOH estimation results begin to show more obvious deviation. The less the number of training cycles, the error of the SOH estimation results of the proposed method will gradually increase. The increase of error is embodied in the second half of battery aging, which increases with the increase of cycle number. It can be seen from the specific error data in Table 2 that although reducing the number of training cycles will reduce the estimation accuracy of SOH, even if only the first quarter of the cycle data are used for network training, the final average estimation error can still be controlled within 4%. Therefore, the proposed method is robust to different training cycle number conditions.

Figure 9 BP neural network fault diagnosis, (a) effect chart of BP neural network training (b) confusion matrix of BP neural network fault diagnosis (see online version for colours)

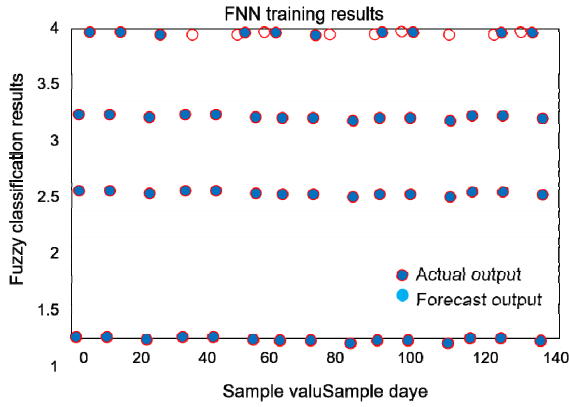


(a)

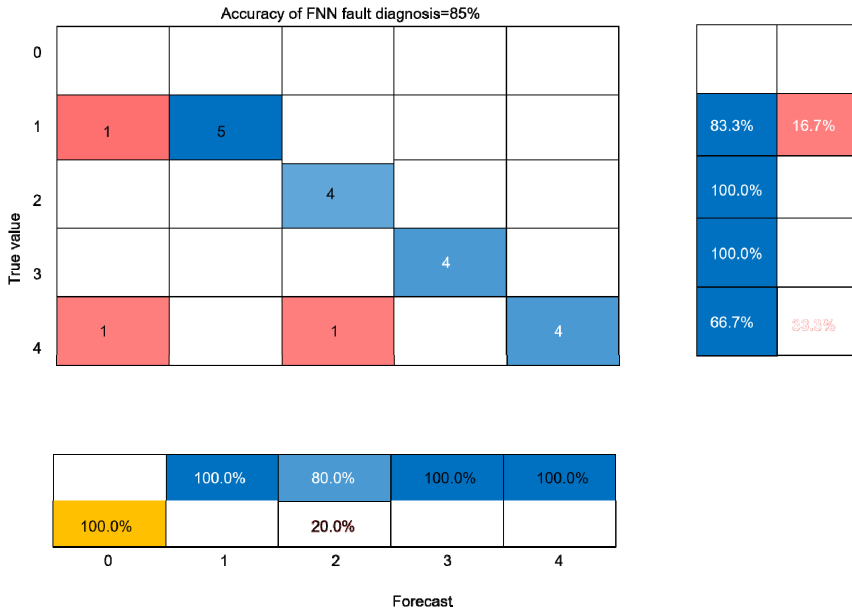


(b)

Figure 10 Fault diagnosis of fuzzy neural network, (a) fuzzy neural network training diagram (b) confusion matrix of fuzzy neural fault diagnosis (see online version for colours)

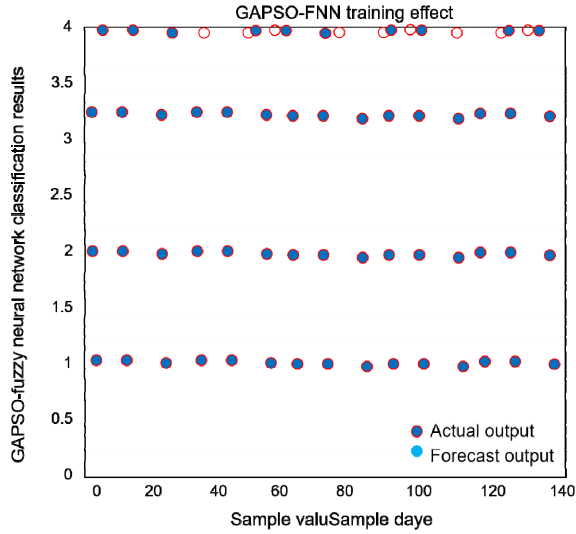


(a)

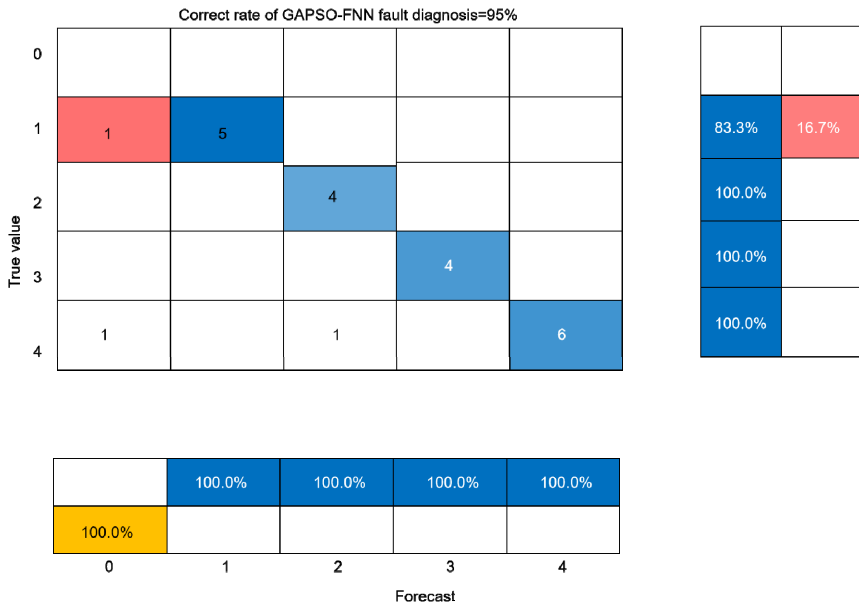


(b)

Figure 11 GAPSO-FNN fault diagnosis, (a) training effect diagram of GAPSO-fuzzy neural network (b) confusion matrix for fault diagnosis of GAPSO-fuzzy neural network (see online version for colours)



(a)

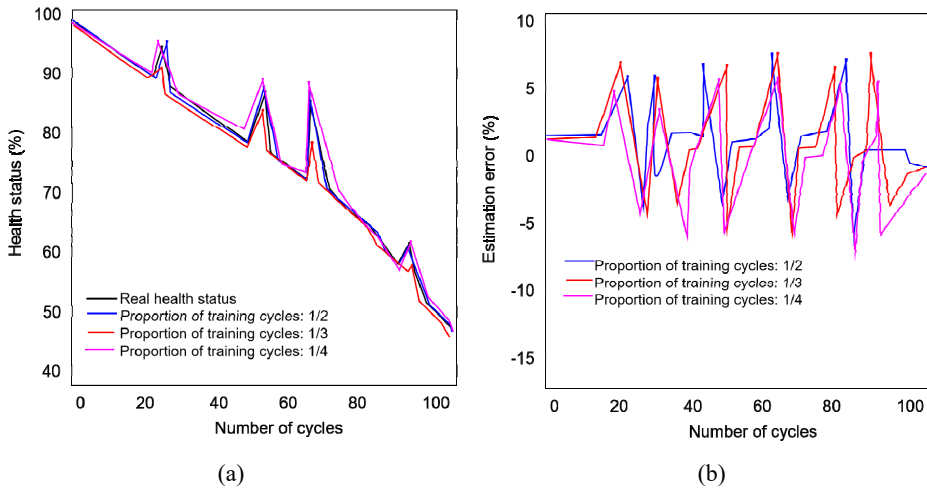


(b)

Table 2 GRA-LSTM health state estimation error

Dataset	MAE (%)	RMSE (%)
1 (1/2)	0.63	0.97
2 (1/2)	0.69	1.20
3 (1/2)	0.95	1.23
2 (1/3)	1.88	2.44
2 (1/4)	2.87	3.87

Figure 12 Experimental results of different training cycles, (a) estimated results (b) error (see online version for colours)



4 Conclusions

This method combines the battery IC curve with LSTM neural network, analyses and extracts the aging characteristics of the battery using the battery charging IC curve, and further trains the LSTM neural network for SOH estimation. In order to improve the training efficiency of the neural network, the GRA method is further introduced to analyse and screen the aging characteristics. The proposed GRA-LSTM method was applied to verify and analyse the battery operation data under three different cycle aging conditions.

Acknowledgements

This work was supported by 2022 Guangxi Education Department of young and middle-aged teachers research basic ability improvement project : Simulation analysis and optimisation of water-cooled radiator based on ANSYS power battery (2022KY1229).

References

- Chen, J. (2019) *Design of Battery Management System based on Lithium Battery Electrochemical Model*, Huaiyin Institute of Technology, DOI: 10.27944/d.cnki.ghygy.2019.000013.
- Chen, S., Yu, W. and Zhu, Y. (2019a) ‘Health diagnosis platform for lithium battery pack of all-electric cruise ship’, *Journal of Jimei University (Natural Science Edition)*, Vol. 24, No. 5, pp.364–370, DOI: 10.19715/j.jmzr.2019.05.07.
- Chen, Y., Bai, Y. and He, Y. (2019b) ‘Comparison of data-driven lithium battery health estimation methods’, *Energy Storage Science and Technology*, Vol. 8, No. 6, pp.1204–1210.
- Chen, Z., Gu, Q., Shen, S., Shen, J. and Shu, X. (2020) ‘Health state prediction of lithium ion batteries based on health feature extraction and PSO-RBF neural network’, *Journal of Kunming University of Technology (Natural Science Edition)*, Vol. 45, No. 6, pp.92–103, DOI: 10.16112/j.cnki.53-1223/n.2020.06.012.
- Duan, Y. (2021) *Life Test and Health State Estimation Of Lithium-Ion Battery*, Zhejiang University, DOI: 10.27461/d.cnki.gzjdx.2021.003144.
- He, F. (2021) *Research on State-of-Charge and State-of-Health Estimation of Lithium-Ion Battery based on Data-Driven*, Xi’an University of Technology, DOI: 10.27398/d.cnki.gxalu.2021.001156.
- Hou, R. and Fan, Q. (2020) ‘Research on health assessment method of lithium ion battery based on convolutional self-coding neural network’, *Computer Measurement and Control*, Vol. 28, No. 8, pp.265–269+275, DOI: 10.16526/j.cnki.11-4762/tp.2020.08.054.
- Li, L., Zhu, Y., Tian, Y., An, Z. and Wang, L. (2019) ‘Research on indirect RUL prediction of lithium ion battery based on Elman neural network’, *Power Technology*, Vol. 43, No. 6, pp.1027–1031.
- Li, X. (2019) *Research on Life Prediction of Lithium Ion Battery based on Neural Network Model*, University of Electronic Science and Technology.
- Li, J. (2020a) *Research on Lithium Battery Health Management under Circuit Fault Diagnosis Method*, Guilin University of Electronic Science and Technology, DOI: 10.27049/d.cnki.gglde.2020.000619.
- Li, X. (2020b) *Research on Health State Estimation Method of Lithium Ion Battery for Energy Storage based on XGB-AKF*, Zhengzhou University, DOI: 10.27466/d.cnki.gzzdu.2020.002658.
- Li, Y., Lei, Q., Wang, H. and Hua, S. (2021) ‘Health status diagnosis of cascade utilization battery based on BP neural network’, *Huadian Technology*, Vol. 43, No. 7, pp.42–46.
- Liang, M. (2022) *Research on Data-Driven Lithium Battery Health State Estimation*, Shandong University of Technology, DOI: 10.27276/d.cnki.gsdgc.2022.000121.
- Liu, G. (2022) *Research on Power Battery Health State Estimation Algorithm based on Patch Learning and Multi-Model Fusion*, Guilin University of Electronic Science and Technology, DOI: 10.27049/d.cnki.gldc.2022.000624.
- Liu, H. (2021) *Research on Residual Service Life Prediction of Lithium Battery based on Improved Neural Network*, Jilin University, DOI: 10.27162/d.cnki.gjlin.2021.004960.
- Lu, S. (2020) *Research on Health Assessment and Residual Life Prediction Methods of Lithium Ion Batteries*, Guangxi University of Science and Technology, DOI: 10.27759/d.cnki.ggxgx.2020.000064.
- Ovshinsky, S.R., Fetcenko, M.A. and Ross, J. (1993) ‘A nickel metal hydride battery for electric vehicles’, *Science*, Vol. 260, No. 5105, pp.176–181.
- Qian, Q. (2021) *Lithium Battery Health Assessment based on Optimized Short-Term and Short-Term Memory Network*, Wuhan University of Science and Technology, DOI: 10.27380/d.cnki.gwkju.2021.000317.

- Ruan, Y. (2020) *Research on Health Assessment Method of Lithium Ion Battery based on Dynamic Impedance Spectroscopy*, Beijing University of Chemical Technology, DOI: 10.26939/d.cnki.gbhgu.2020.001144.
- Surya, S., Rao, V. and Williamson, S.S. (2021) 'Comprehensive review on smart techniques for estimation of state of health for battery management system application', *Energies*, Vol. 14, No. 15, p.4617.
- Tan, Q. and Wei, J. (2021) 'Lithium ion battery health assessment based on deep convolution neural network', *Proceedings of the 22nd China Annual Conference on System Simulation Technology and Applications (CCSSTA22nd 2021)*, pp.282–287, DOI: 10.26914/c.cnkihy.2021.059255.
- Wang, B., Chen, D., Zhang, J., Zhang, Z., Ma, X. and Zhang, Z. (2022) 'Research on health status of large-scale battery based on space-time distribution mapping', *Smart Power*, Vol. 50, No. 6, pp.85–91.
- Wang, F. (2020) *Research on SOH Prediction of Lithium Battery based on LSTM Neural Network*, Chongqing University of Posts and Telecommunications, DOI: 10.27675/d.cnki.gcydx.2020.000919.
- Wang, P. (2022a) *Research on Extraction of Health Factors and Prediction of Residual Life of Lithium Ion Batteries*, Hunan University of Technology, DOI: 10.27730/d.cnki.glhngy.2022.000469.
- Wang, X. (2022b) *Research on Health State Estimation and Residual Life Prediction of Lithium Ion Batteries*, Liaoning University of Engineering and Technology, DOI: 10.27210/d.cnki.glnju.2022.000519.
- Wang, Y., Liu, X. and Gao, D. (2021) 'SOH estimation and RUL prediction of lithium battery based on BiLSTM neural network', *Electronic Measurement Technology*, Vol. 44, No. 20, pp.1–5, DOI: 10.19651/j.cnki.emt.2107683.
- Wang, Z. (2019) *Research on RUL Prediction Method of Lithium Ion Battery based on Neural Network*, Central North University.
- Wei, Z., Han, X. and Li, X. (2022) 'Health assessment of cascade utilization battery based on deep neural network', *Journal of Solar Energy*, Vol. 43, No. 5, pp.518–524, DOI: 10.19912/j.0254-0096.tynxb.2022-0550.
- Xu, H. (2020) *Research on Electromagnetic Radiation Signal Recognition and Battery Health Prediction Technology based on Deep Learning*, Beijing University of Posts and Telecommunications, DOI: 10.26969/d.cnki/gbydu.2020.001683.
- Xue, T., Zhang, C., Yan, L., Wu, J. and Jin, Y. (2022) 'Health state estimation of lithium ion battery based on WOA-BP neural network', *Shandong Electric Power Technology*, Vol. 49, No. 10, pp.16–22+37.
- Yao, Y., Chen, Z., Wu, L., Cheng, S. and Lin, P. (2021) 'A method of lithium ion battery health state estimation based on improved grid search and generalized regression neural network', *Electrical Technology*, Vol. 22, No. 7, pp.32–37.
- Zeng, W. (2019) *Health Assessment and Residual Life Prediction Method of Lithium Ion Battery*, Anhui University of Technology.
- Zhang, S. (2022) *Research on the State of Charge and Health Prediction of Lithium Battery based on Machine Learning*, Guangxi Normal University, DOI: 10.27036/d.cnki.ggxsu.2022.001431.
- Zhang, Z. (2021) *Online Monitoring of Lithium Battery Health based on Improved Long-Term and Short-Term Memory Neural Network*, Chongqing University of Posts and Telecommunications, DOI: 10.27675/d.cnki.gcydx.2021.000848.
- Zheng, Y., Wen, H., Han, F. and Yang, X. (2019) 'Prediction of battery health status based on particle swarm neural network based on external characteristics of battery', *Science and Technology and Engineering*, Vol. 19, No. 36, pp.184–189.

- Zhou, C. and Wang, Y. (2020) 'Lithium battery health state estimation based on automatic encoder feature extraction', *Proceedings of the 21st China Annual Conference on System Simulation Technology and its Applications (CCSSTA21st 2020)*, pp.255–259, DOI: 10.26914/c.cnkiyh.2020.021696.
- Zhou, C., Wang, Y., Li, K. and Chen, Z. (2022) 'Health state estimation of lithium-ion battery based on grey correlation analysis – short and long term memory neural network', *Journal of Electrical Technology*, Vol. 37, No. 23, pp.6065–6073, DOI: 10.19595/j.cnki.1000-6753.tces.211366.
- Zhou, R. (2022) *Research on Power Battery Health State Estimation Algorithm based on Actual Operation Data of Electric vehicles*, Guilin University of Electronic Science and Technology, DOI: 10.27049/d.cnki.gglc.2022.000720.